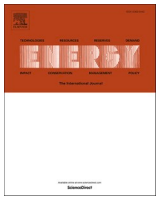
Energy 344 (2026) 139724



Contents lists available at ScienceDirect

Energy

journal homepage: www.elsevier.com/locate/energy





Comprehensive comparative assessments of optimal distributed solar-energy systems for combined heat and power

Jingyuan Xu [a,b], Jian Song [a,c], Gan Huang [a,b], Matthias Mersch [a], Kai Wang [a,d], Christos N. Markides [a,*]

[a] Clean Energy Processes (CEP) Laboratory, Department of Chemical Engineering, Imperial College London, South Kensington Campus, London SW7 2AZ, United Kingdom
[b] Institute of Microstructure Technology, Karlsruhe Institute of Technology, Karlsruhe 76344, Germany
[c] Birmingham Centre for Energy Storage & School of Chemical Engineering, University of Birmingham, Birmingham B15 2TT, United Kingdom
[d] Institute of Refrigeration and Cryogenics, Zhejiang Key Laboratory of Refrigeration and Cryogenic Technology, Zhejiang University, Hangzhou 310027, China

ARTICLE INFO

Keywords:
Distributed energy systems
Multi-objective optimisation
Photovoltaics (PV)
Photovoltaic thermal (PVT)
Solar energy
Solar thermal

ABSTRACT

In this paper, we present the results of techno-economic evaluations of a range of optimised solar energy systems for heat and/or power provision in buildings located in hot, solar-rich climatic regions. Hybrid photovoltaic–thermal (PVT), solar thermal (ST), photovoltaic (PV), and combined PV and ST (PV-ST) systems are assessed using annual simulations. The systems are evaluated for electricity generation, space heating, and domestic hot water supply for a hotel in Fayoum, Egypt, which serves as a representative case study. Multi-objective optimisations are conducted to maximise the annual energy-saving ratio while minimising the payback time. For each technology, four representative commercial products with a spread of performance and cost characteristics are selected for comparison. The results demonstrate that detailed techno-economic assessments are essential for identifying the most economical solution, as relying solely on systems with the lowest upfront cost can be misleading. Energetic analyses show that, for a constrained maximum installation area of 150 m^2, the best-performing PVT system outperforms the alternatives in terms of energy savings. Specifically, it achieves a maximum annual energy-saving ratio of 43 % across the available area. The economic assessments show that the proposed systems are profitable in the specified case study, i.e., payback $<$ 25 years, if appropriately sized and operated. For the same energy savings, the PVT systems are the most profitable with the shortest payback time (min. 6.2 years) and lowest levelised cost of electricity (min. 0.028 $/kWh), thanks to their lower investment costs per unit displaced energy. The payback time and levelised cost PV-ST systems (min. 8.1 years, 0.036 $/kWh) are close to those of ST systems (min. 8.1 years, 0.035 $/kWh), while PV systems are less attractive in this context (min. 8.6 years, 0.041 $/kWh). From an environmental perspective, the CO_2 emission reduction potential of PVT systems is considerably higher (by 20–52 %) than those of all other systems, reaching a maximum of 31 tCO_2/year. The proposed systems, especially the PVT systems, show excellent decarbonisation potential and cost effectiveness, thus motivating further development for applications in buildings in such climate zones.

1. Introduction

Heating, cooling, and electricity are essential energy demands in buildings and together account for over one-third of global final energy consumption and nearly 40 % of global CO_2 emissions [1]. The overall vision of most national strategies is to achieve sustainable energy provision, while reducing energy-related emissions, pollution, fossil-fuel consumption, and dependence on fossil resources. To achieve the goals set out in the Paris Agreement, the total share of renewable energy is required to rise from around 15 % of the total primary energy supply in 2015 to around two-thirds by 2050 [2].

Solar energy is one of the cleanest and most abundant renewable energy sources. Currently established solar energy harvesting technologies include photovoltaic (PV) modules and solar thermal (ST) collectors that convert solar radiation either into electricity or thermal energy. Hybrid photovoltaic-thermal (PVT) systems are a promising emerging

* Corresponding author.
E-mail address: c.markides@imperial.ac.uk (C.N. Markides).

https://doi.org/10.1016/j.energy.2025.139724
Received 23 June 2025; Received in revised form 15 December 2025; Accepted 17 December 2025
Available online 23 December 2025
0360-5442/© 2025 The Authors. Published by Elsevier Ltd. This is an open access article under the CC BY license (http://creativecommons.org/licenses/by/4.0/).

solar technology that is able to cogenerate electricity and thermal energy from the same collector area [3].

Such systems combining electricity and heat generation are particularly interesting for applications with both electrical and thermal demands. One representative example is hotels, which require electricity, space heating and cooling, as well as hot water provision. Hotels in regions with high solar irradiation are particularly interesting for solar energy applications, though systems need to be designed carefully to maximise economic and environmental benefits. Therefore, in this study, we optimise solar energy systems for a hotel located in Fayoum, Egypt. Different system options (PV, ST, and PVT) are compared within a holistic framework, with a focus on economic and environmental trade-offs.

PV modules are the most well-established solar technology. They convert solar energy directly into electricity, and have low installation complexity and costs [4,5]. The global cumulative installed PV capacity exceeded 1.5 TW at the end of 2023, which is an increase by a factor of ~7 from 230 GW in 2015 [6]. Global capacity is predicted to exceed 8 TW by 2050 [7]. This exponential growth can be largely attributed to dramatic cost reductions: from 2010 to 2019, the global levelised cost of electricity (LCOE) for utility-scale PV dropped by 82 % [8]. Monocrystalline Silicon (c-Si) and polycrystalline Silicon (p-Si) are the most commonly used materials in commercial PV modules, with the former offering slightly higher efficiencies but also higher costs than the latter. In addition to large utility-scale PV systems, small-scale rooftop and building-integrated PV systems have attracted considerable interest in recent years. In this context, PV modules can be coupled with reversible heat pumps for combined provision of heating, cooling, and electricity [9]. A range of energy storage technologies [10], solar tracking systems [11], and operational control strategies [12] have been proposed to improve the performance of solar PV systems. One limitation of PV modules is their relatively low efficiency (only 15 %–23 % for commercial Si PV modules), with most of the incident solar energy being dissipated as waste heat (> 70 %). Especially in hot, sunny conditions, this leads to a significant increase in their operating temperature and a deterioration in efficiency.

ST collectors to supply thermal energy for use in buildings and industrial facilities are another mature solar technology. Heat is required at different temperature levels depending on the application. Flat-plate, glazed ST collectors are relatively affordable and operate with reasonable efficiencies for outlet temperatures up to 80–100 °C [13]. Evacuated-tube collectors are considered a better option for heat provision with required temperatures above 100 °C and up to 150 °C [13]. These two ST collector types are particularly suitable for domestic hot water [14] and space heating [15] applications. Concentrated ST collectors, on the other hand, can reach temperatures over 200 °C, which is considered suitable for power generation via heat-to-power conversion technologies [16]. The inclusion of thermal storage [17] allows ST systems to cover significant shares of the energy demand, by enabling a reduction in the discordance (in time or rate) between the availability of energy and its consumption. ST technologies can be further integrated with thermally-driven cooling technologies, typically sorption chillers [18–20], to reduce the amount of electricity consumed by cooling equipment.

Hybrid PVT systems [3,21], which combine the capabilities of PV and ST systems, produce electricity and useful heat simultaneously from the same area. A PVT collector typically consists of PV cells attached to a thermal absorber. The thermal absorber recovers heat from the PV cells as useful thermal energy and simultaneously cools the PV cells, resulting in higher overall efficiencies and larger energy yields per unit area than separate, standalone PV or ST systems [22], which is particularly important if the area for installation is limited. The PVT market has seen significant global growth of ~10 % on average per year in 2018 and 2019, with a higher growth rate of 14 % in the European market [23]. PVT collectors can be categorised into glazed and unglazed designs, according to the presence of a glass cover to reduce heat losses. Extensive research has focused on PVT-based combined heat and power (CHP) systems for applications in sports centres [15], residential dwellings [14], dairy farms [24], and other buildings [18,19]. Results have shown that the deployment of PVT systems can lead to significant decarbonisation, with a reasonable payback time. The integration of PVT collectors with cooling technologies [25], desalination technologies [26,27], heat pumps [28,29], or organic Rankine cycles (ORCs) [30], further allows such systems to match wider energy-system demands and to increase their solar contribution. Recent research has focused on absorber-exchanger designs [31], spectral splitting concepts [32,33], and nanofluid coolants [34], which have emerged as promising solutions for performance enhancement.

The selection of high-efficiency cost-competitive solutions in various applications is of particular interest. Mousa et al. [35] performed comparative energy and emission assessments on solar PV and ST systems for industrial applications at 12 locations around the world. Their results revealed that the payback time of ST systems is shorter than that of PV systems in high irradiation locations, but longer in low irradiation locations. Behar et al. [36] performed techno-economic assessments of PV systems, concentrated ST power systems, and a combination of the two (PV-ST) for mining processes. The study indicated that PV systems are the most suitable technology since its LCOE is about four times lower than that of ST power systems, and 50 % that of the combined system. Other techno-economic comparisons of three solar-assisted heat pump systems based on PV, ST, and combined PV-ST arrays were conducted for residential buildings [37]. It was found that PV-assisted heat pump systems can outperform the alternatives when considering energetic and economic performance. The energetic and economic performance of a concentrated combined PV-ST system and a standalone concentrated PV system were also compared in Ref. [38]. The results showed that combined PV-ST systems can improve LCOE by up to 16 %, respectively, compared to standalone PV systems. Good et al. [39] performed a comparison of the energy performance of standalone PV, combined PV-ST, and PVT systems for a net-zero energy building. The results suggested that the PV system gets closest to reaching a net-zero energy balance in comparison to other systems. A further study [15] compared the techno-economic potential of PV, ST, combined PV-ST, and PVT systems for energy provision to sports centres. The results showed that the PVT system outperforms the other alternatives in terms of total energy output and CO_2 emissions, covering 82 % of the electricity demand and 51 % of the thermal demand, while the PV system outperforms the rest of the investigated solutions in terms of payback time (9.4 years *vs.* > 14 years).

Most studies of solar cogeneration systems are focused on the well-established technological options, *i.e.*, PV, ST, or combined PV-ST systems, with fewer considering emerging PVT technologies. In these studies, comparisons are usually performed of different systems based on fixed parameter values (*e.g.*, fixed installation areas) that are selected to be the same for different systems, making it difficult to fully understand (and compare) the respective optimal performance of each system. Even when optimisation is performed, studies in the literature are often limited to energetic performance. Comprehensive multi-objective optimisation approaches that also account for economic and environmental performance remain scarce. The current state-of-the-art in the literature reveals a lack of uniform, common approaches for the holistic comparison of both established and emerging solar systems from multiple perspectives. Furthermore, comparative studies of different solar systems are almost invariably restricted to a single technological design option, or commercially-available product, which are assumed to be representative of each solar technology. Given the breadth and diversity of design options and commercial products on the market with different performance and cost characteristics, investigating a wide range of characteristics for each technology is crucial for robust comparisons and reliable technology selection.

This paper aims to fill the aforementioned knowledge gaps and to provide a uniform common approach for a holistic comparison of

established and emerging solar systems considering multiple evaluation criteria including energetic and economic performance, and environmental potential. Detailed cost modelling is included in a holistic comparison framework for solar energy systems. Multi-objective optimisation using a nondominated sorting genetic algorithm-II (NSGA-II) [40] is performed to compare four types of solar systems, *i.e.*, PV-based solar-power systems, ST-based solar-thermal systems, combined PV-ST solar-CHP systems, and hybrid PVT-based solar-CHP systems. For each solar technology, a variety of commercial products are studied and compared. A key contribution is the identification of trade-offs between performance and payback time of the different systems.

In what follows, the optimisation methodology is first introduced in Section 2, followed by a description of the input data such as meteorological data and energy demands in Section 3. The performance of the solar systems while aiming at covering the hot water, space heating, and electricity demands in the selected case study of a hotel in Egypt is then analysed and compared in Sections 4 and 5. Finally, key observations and conclusions from the study are summarised in Section 6.

2. Methodology

2.1. Calculation models

Transient models are developed for the four solar system configurations: hybrid PVT-based solar CHP, ST-based solar thermal, PV solar power, and combined PV–ST solar CHP. All models are implemented in MATLAB. They account for both electrical and thermal performance, as well as interactions between generation, storage, and demand. Simulations are performed at 30-min time steps over a full year using local weather data and a measured building-demand profile. We first describe the PVT-based CHP model, which is the most comprehensive of the four. The ST, PV, and PV–ST system models are then presented by referencing the relevant sub-models and equations introduced for the PVT system.

2.1.1. Hybrid PVT-based solar CHP system

The proposed hybrid PVT-based CHP system is shown in Fig. 1. The system comprises PVT collectors, a hot water storage tank, an external auxiliary electrical heater, a bypass branch, a mixing device, a circulation pump, and thermally insulated connection pipes. The generated electricity is directly used for covering the electricity demand, or it is fed into the grid using net metering when the power generation exceeds the demand. The thermal energy collected by the PVT collectors is transferred to the hot-water tank via a circulating heat-transfer fluid, enabling heat availability during periods of low irradiation (e.g., at night). The hot water is delivered to the end-user by circulating water directly from the water storage tank. The bypass branch controls the collector outlet temperature and ensures that the fluid entering the tank contributes to heating the stored water [14]. The circulation of the heat transfer fluid is regulated by a controller that activates the circulation pump. An external auxiliary electric heater is required to upgrade the thermal output of the system, typically in winter, to ensure that the output temperature of the water tank reaches the required value. The mixing device is used to cool down the delivered water by mixing it with mains water, typically in summer, in case the hot water temperature exceeds the set-point temperature.

The PVT collector is modelled as a lumped component based on thermal and electrical efficiency curves. This modelling strategy is mentioned in the European Standard EN 12975 [41] and has been widely used in existing literature [42,43]. The efficiency curve is obtained by testing the collector over a range of inlet temperatures while maximising the energy output at each operating condition. The instantaneous thermal efficiency of the PVT collector is determined from:

$$\eta_{th}\dot{m}_f c_f\left(\frac{T_{fo}-T_{fi}}{GA}\right)=\eta_0-a_1T_r-a_2GT_r^2 \tag{1}$$

$$T_r=\frac{T_{fm}-T_a}{G} \tag{2}$$

where $\dot{m}_f$, c_f, G and A are the mass flow rate through the collector, the specific heat of the fluid, the total solar irradiance, and the collector area, T_{fo} and T_{fi} are the fluid temperatures at the outlet and inlet of the collector, T_r, T_{fm} and T_a are the reduced temperature, the mean fluid temperature between inlet and outlet temperature of the collector, and the ambient temperature, and η_0, a_1 and a_2 are the thermal efficiency, first-order heat loss coefficient, and second-order heat loss coefficient, respectively, which are determined by plotting the instantaneous thermal efficiency against the reduced temperature and applying a second order least-squares fit to the data. These coefficients vary for different collectors due to different manufacturing quality, absorber design, etc.

The instantaneous electrical efficiency of PVT collectors is defined as:

$$\eta_{el}=\frac{\dot{E}}{GA}=\eta_{ref}\left[1+\beta\left(T_{ce}-T_{ref}\right)\right] \tag{3}$$

where $\dot{E}$ is the generated electrical power, T_{ce} the PV cell temperature, assumed to be the same as T_{fm} in the model, β the temperature coefficient, and η_{ref} the reference electrical efficiency at a reference collector temperature T_{ref} of 25 °C and a solar irradiance of 1000 W/m^2.

The water storage tank is modelled as a fully mixed tank, neglecting the influence of stratification on the overall performance. As discussed in Section 5.4, this likely leads to a slightly conservative estimation of

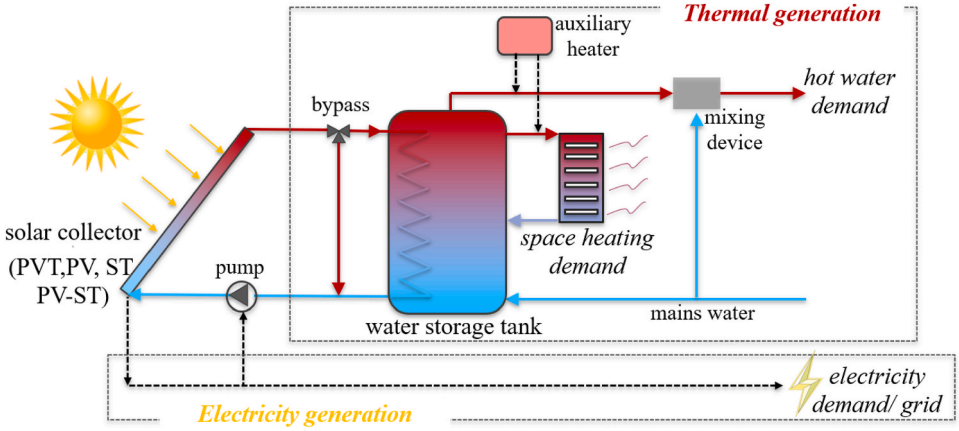


Fig. 1. Schematic diagram of solar heating and/or power systems. The PV system only includes the electricity generation, the ST system only the thermal energy generation, and the PVT system and PV-ST system both, the thermal energy and electricity generation.

the potential of ST systems. The energy balance equation for the water storage tank is:

$$M_t c_w \frac{dT_{wt}}{dt} = \dot{Q}_{coil} - \dot{Q}_{loss} - \dot{Q}_{cov,hw} - \dot{Q}_{cov,sh} \quad (4)$$

The above energy equation accounts for: (i) the heat delivered from the solar collectors via the immersed heat exchanger, $\dot{Q}_{coil}$, (ii) the heat losses of the water tank to the surroundings, $\dot{Q}_{loss}$ (iii) the hot water demand covered by the water storage tank, $\dot{Q}_{cov,hw}$, (iv) the space heating demand covered by the water storage tank, $\dot{Q}_{cov,sh}$. Here, M_t and c_w are the water mass and specific heat capacity respectively, and T_{wt} is the water temperature in the tank.

The heat delivered to the water tank via the immersed coil heat exchanger, $\dot{Q}_{coil}$, is calculated using the effectiveness-NTU method:

$$\dot{Q}_{coil} = \epsilon_{hx} \dot{m}_f c_f (T_{fo} - T_{wt}) \quad (5)$$

where ε_{hx} is the heat transfer effectiveness of the coil heat exchanger inside the tank. The relation between the heat exchanger effectiveness ε_{hx} and NTU is [44]:

$$\epsilon_{hx} = 1 - e^{-NTU} \quad (6)$$

$$NTU = \frac{A}{\dot{m}_f c_f R_{coil}} \quad (7)$$

The thermal resistance R_{coil} accounts for the forced convection in the coil, the free convection in the tank, and the thermal resistance of the pipe walls:

$$R_{coil} = \frac{d_o}{d_i h_{coil}} + \frac{\ln\left(\frac{d_o}{d_i}\right)}{2k_p} + \frac{1}{h_t} \quad (8)$$

where d_o, d_i and k_p are the outside diameter of the coil, inside diameter of the coil, and thermal conductivity of the pipe, h_{coil} is the heat transfer coefficient for the forced convection in the coil, and h_t the heat transfer coefficient for the free convection in the tank. The correlations used for the calculation of h_{coil} for forced laminar [45] and turbulent [46] convection in the helical coil are:

$$h_{coil} = \frac{Nu_{coil} k_{coil}}{d_i} \quad (9)$$

$$Nu_{coil} = \begin{cases} 3.66 + 0.08\left[1 + 0.8\left(\frac{d_i}{d_o}\right)^{0.9}\right]\left[(Re_{coil})^m Pr^{0.3}\right] & Re_{coil} < Re_c \\ 0.023(Re_{coil})^{0.85} Pr^{0.4} & Re_{coil} > Re_c \end{cases} \quad (10)$$

where:

$$m = 0.5 + 0.29\left(\frac{d_i}{d_o}\right)^{0.1} \quad (11)$$

$$Re_c = 2300\left[1 + 8.6\left(\frac{d_i}{d_o}\right)^{0.45}\right] \quad (12)$$

The heat transfer coefficient h_t is calculated using the following correlation [47]:

$$h_t = \frac{Nu_t k_t}{d} \quad (13)$$

$$Nu_t = 0.49(Ra_t)^{0.26} \quad (14)$$

The heat losses of the water tank to the surroundings, $\dot{Q}_{loss}$, is given by:

$$\dot{Q}_{loss} = A_{wt} h_{wt,loss} (T_{wt} - T_a) \quad (15)$$

where A_{wt} is the surface area of the water tank, and $h_{wt,loss}$ is the heat loss coefficient.

When the water temperature in the tank is higher than the required hot water temperature, all the hot water demand can be covered by the water storage tank, and mains water will be mixed with the tank water to reach the required temperature. When the tank water temperature is between the required hot water temperature and the mains water temperature, only a part of the demand can be covered by the water storage tank, and the auxiliary electrical heater is used to increase the temperature of the tank water. When the tank water temperature is lower than or equal to the mains water temperature, no hot water demand can be covered by the water storage tank and the auxiliary heater provides all necessary energy. The hot water demand covered by the water storage tank, $\dot{Q}_{hw,cov}$, is therefore calculated from:

$$\dot{Q}_{hw,cov} = \begin{cases} \dot{Q}_{hw,dem} & T_{wt} \geq T_{hw,dem} \\ \left(\frac{T_{wt} - T_{mains}}{T_{hw,dem} - T_{mains}}\right)\dot{Q}_{hw,dem} & T_{mains} < T_{wt} < T_{hw,dem} \\ 0 & T_{wt} \leq T_{mains} \end{cases} \quad (16)$$

where $\dot{Q}_{hw,dem}$ is the hot water demand, $T_{hw,dem}$ the required delivery temperature of the hot water, and T_{mains} the temperature of the mains water.

Similarly, the space heating demand covered by the water storage tank, $\dot{Q}_{sh,cov}$, is given by:

$$\dot{Q}_{sh,cov} = \begin{cases} \dot{Q}_{sh,dem} & T_{wt} \geq T_{sh,dem} \\ \left(\frac{T_{wt} - T_{sh,out}}{T_{sh,dem} - T_{sh,out}}\right)\dot{Q}_{sh,dem} & T_{sh,out} < T_{wt} < T_{sh,dem} \\ 0 & T_{wt} \leq T_{sh,out} \end{cases} \quad (17)$$

where $\dot{Q}_{sh,dem}$ is the space heating demand, $T_{sh,dem}$ the required delivery temperature of the space heating, and $T_{sh,out}$ the temperature at the outlet of the radiator for space heating.

If we neglect heat losses from the pipes between the collector and tank, we obtain:

$$T_{fi} = T_{fo} - \epsilon_{hx}(T_{fo} - T_{wt}) \quad (18)$$

The electrical power consumed by the circulation pump is:

$$\dot{W}_{pump} = \frac{\dot{m}_f \Delta P}{\eta_p \rho_f} \quad (19)$$

where η_p is the pump efficiency, assumed to be 65 % in the model [21], and ρ_f is the density of the fluid. The pressure drop ΔP accounts for pressure losses through the pipework ΔP_{pi} and the collector ΔP_c. The friction factor that determines the pipe pressure loss, ΔP_{pi}, is calculated from Ref. [48]:

$$\Delta P_{pi} = \frac{8 \dot{m}_f^2 L_p f}{\pi^2 \rho_w D^5} \quad (20)$$

$$f = \begin{cases} 0.316 Re^{-0.25} & Re < 2 \times 10^4 \\ 0.184 Re^{-0.20} & Re \geq 2 \times 10^4 \end{cases} \quad (21)$$

where L_p and D are the pipe length and diameter, and Re is the Reynolds number based on D.

The pressure losses through the solar collector, ΔP_c, are given by Ref. [49]:

$$\Delta P_c = A_c\left(21.77 \dot{m}_f^2 + 3.54 \dot{m}_f\right) \quad (22)$$

where A_c is the area of the solar collectors.

For the auxiliary heater, the additional thermal energy required for hot water ($\dot{Q}_{hw,aux}$) and for space heating ($\dot{Q}_{sh,aux}$) are given by:

$$\dot{Q}_{hw,aux} = \begin{cases} 0 & T_{wt} \geq T_{hw,dem} \\ \left(\frac{T_{hw,dem} - T_{wt}}{T_{hw,dem} - T_{mains}}\right)\dot{Q}_{hw,dem} & T_{mains} < T_{wt} < T_{hw,dem} \\ \dot{Q}_{hw,dem} & T_{wt} \leq T_{mains} \end{cases} \quad (23)$$

$$\dot{Q}_{sh,aux} = \begin{cases} 0 & T_{wt} \geq T_{sh,dem} \\ \left(\frac{T_{sh,dem} - T_{wt}}{T_{sh,dem} - T_{sh,out}}\right)\dot{Q}_{sh,dem} & T_{sh,out} < T_{wt} < T_{sh,dem} \\ \dot{Q}_{sh,dem} & T_{wt} \leq T_{sh,out} \end{cases} \quad (24)$$

Eqs. (1)–(24) are solved iteratively with a time step of 30 min over a year, using local weather data for the site in Egypt and a measured energy demand profile from the hotel building. Then, the half-hourly transient operations of the systems can be obtained, which can be used to further evaluate the energetic, economic and environmental potentials of the systems.

The main technical specifications of the PVT collectors are given in Table 1. Four typical commercial PVT collectors from different manufacturers are studied and compared: a glazed PVT collector with a sheet-and-tube absorber made of aluminium (PVT-1 [50]), a glazed PVT collector with a flat-box absorber made of polycarbonate (PVT-2 [50]), a glazed PVT collector with a sheet-and-tube absorber made of copper (PVT-3 [25]), and an unglazed PVT collector with a roll-bond absorber made of aluminium (PVT-4 [25]).

2.1.2. ST-based solar thermal system

The configuration of the ST-based system is the same as the thermal generation part in Fig. 1, but there is no electricity generation. The system description and working principle are similar to that of the thermal generation part of the PVT system described in Section 2.1.1. Since the ST-based solar system only generates thermal energy for meeting the hot water and space heating demands, the electricity demand is met purely by grid electricity. The thermal demand not satisfied by the ST-based solar system is provided by the auxiliary electrical heater. The ST collectors are modelled based on their thermal efficiency curves (Eqs. (1) and (2)). The water storage tank is modelled based on Eqs. (4)–(18). Eqs. (19)–(22) are used to model the pump in the solar collector circuit. The additional thermal energy required for the auxiliary electrical heater is given by Eqs. (23) and (24).

In this study we compare four typical commercial ST collectors described in Table 1: a low-cost evacuated tube collector (ST-1 [51]), a high-cost evacuated tube collector (ST-2 [52]), a low-cost flat-plate collector (ST-3 [53]), a high-cost flat-plate collector (ST-4 [54]). These collectors were chosen based on a market analysis [55], with the aim to represent the full spectrum of cost and efficiency of the two relevant ST collector types.

2.1.3. PV solar power system

The configuration of the PV solar power system is the same as the electricity generation part in Fig. 1, and there is no thermal energy generation. The electricity generated by PV modules is directly used to cover the electricity demand of the hotel, and the excess electricity is fed into the grid, using net metering. The electricity demand not covered by the PV system is provided by the electricity grid. The electrical heater is used as a backup system for space heating and hot water.

The PV modules are modelled using the electrical-efficiency relation given in Eq. (3). Four alternative commercial PV modules are proposed (see Table 1): a low-cost c-Si silicon module (PV-1 [56]), a high-cost c-Si silicon module (PV-2 [57]), a low-cost p-Si silicon module (PV-3 [58]), a high-cost polycrystalline silicon module (PV-4 [59]). Similar to the ST collectors, these modules were chosen to represent the range of PV modules currently available on the market [55].

2.1.4. Combined PV-ST solar CHP system

Combined PV-ST system configurations feature side-by-side combinations of PV and ST systems. Unlike the hybrid PVT systems that generate both heat and power from the same collector area, in combined PV-ST systems the heat and power are generated separately from ST collectors and PV modules, respectively. The models of the combined

Table 1
Main technical specifications of PVT collector, solar thermal (ST) collector and PV module.

Collector	Parameter	Value			
PVT		PVT-1 [50]	PVT-2 [50]	PVT-3 [25]	PVT-4 [25]
	Area per collector, m^2	1.55	1.55	1.61	1.63
	Absorber-exchanger type	sheet-and-tube	flat-box	sheet-and-tube	roll-bond
	Absorber-exchanger material	aluminium	polycarbonate	copper	aluminium
	Glass cover	covered	covered	covered	uncovered
	Nominal power, W_p	240	240	260	300
	Reference electrical efficiency (η_{ref})	15 %	15 %	16 %	18 %
	Temperature coefficient (β), 1/K	-0.45 %	-0.45 %	-0.47 %	-0.39 %
	Intercept thermal efficiency (η_0)	70 %	73 %	51 %	47 %
	1st-order heat loss coefficient (a_1)	3.9	3.3	4.9	9.5
	2nd-order heat loss coefficient (a_2)	0.015	0.018	0.021	0
	Price, $/collector	450	360	590	440
ST		ST-1 [51]	ST-2 [52]	ST-3 [53]	ST-4 [54]
	Area per collector, m^2	3.1	3.26	2.09	2.51
	Collector type	evacuated tube	evacuated tube	flat plate	flat plate
	Intercept thermal efficiency (η_0)	39 %	63 %	71 %	77 %
	1st-order heat loss coefficient (a_1)	0.88	0.93	3.8	3.5
	2nd-order heat loss coefficient (a_2)	0.012	0.0040	0.011	0.0083
	Price, $/collector	500	1500	520	790
PV		PV-1 [56]	PV-2 [57]	PV-3 [58]	PV-4 [59]
	Area per collector, m^2	1.63	1.73	1.65	2.01
	Cell type	c-Si	c-Si	p-Si	p-Si
	Nominal power, W_p	290	370	280	360
	Reference electrical efficiency (η_{ref})	17 %	21 %	17 %	18 %
	Temperature coefficient (β), 1/K	-0.40 %	-0.30 %	-0.40 %	-0.36 %
	Price, $/collector	190	430	160	240
PV-ST	Combination	PV1-ST1	PV1-ST2	PV1-ST3	PV1-ST4

PV-ST system are based on the ST system model described in Section 2.1.2 and the PV system model in Section 2.1.3. As shown in Table 1, four sets of combinations of PV and ST products are considered, namely PV1-ST1, PV1-ST2, PV1-ST3 and PV1-ST4. The total cumulative area of the PV modules and ST collectors is kept equal to the other systems, while different areas are optimally allocated for PV modules and ST collectors.

2.2. System performance indicators

The comprehensive assessments of the solar-based systems are based on multiple evaluation criteria, including energetic performance, economic analysis, and environmental benefits.

2.2.1. Energetic performance

The fraction of energy demand (in the form of heat or power) covered by the solar-based systems over a year is a crucial energy performance indicator. The fraction of the annual hot water demand covered $f_{\mathrm{hw,cov}}$, the fraction of the annual space heating demand covered $f_{\mathrm{sh,cov}}$, and the fraction of the annual electricity demand covered $f_{\mathrm{el,cov}}$, are:

$$f_{\mathrm{hw,cov}} = \frac{Q_{\mathrm{hw,cov}}}{Q_{\mathrm{hw,dem}}} \tag{25}$$

$$f_{\mathrm{sh,cov}} = \frac{Q_{\mathrm{sh,cov}}}{Q_{\mathrm{sh,dem}}} \tag{26}$$

$$f_{\mathrm{el,cov}} = \frac{E_{\mathrm{cov}}}{E_{\mathrm{dem}}} \tag{27}$$

where $Q_{\mathrm{hw,dem}}$, $Q_{\mathrm{sh,dem}}$ and E_{dem} are the annual hot water, space heating and electricity demands, and $Q_{\mathrm{hw,cov}}$, $Q_{\mathrm{sh,cov}}$ and E_{cov} are the annual hot water, space heating and electricity demands that are covered by the proposed solar systems, respectively.

Another key indicator is the annual energy saving relative to a conventional reference system consisting of an electric heater for hot water, a heat pump for space heating, and grid electricity for power. The annual energy saving E_{s} is the sum of the actual electricity output from the solar collector and the corresponding electricity required for the thermal output all over a full year, *i.e.*:

$$E_{\mathrm{s}} = E_{\mathrm{cov}} + \frac{Q_{\mathrm{hw,cov}}}{\eta_{\mathrm{eh}}} + \frac{Q_{\mathrm{sh,cov}}}{COP_{\mathrm{hp}}} \tag{28}$$

where η_{eh} and COP_{hp} are the efficiency of the electrical heater and coefficient of performance of the heat pump, respectively. The efficiency of the electrical heater (η_{eh}) is taken here to be 98 % [60]. The coefficient of performance of the heat pump (COP_{hp}) is taken from the fitted performance curve based on the manufacturers' datasheets of 13 commercial air-source heat pump products with an ambient air temperature of 27 °C for space heating:

$$COP_{hp} = 2.7308e^{0.0153T_{\mathrm{a}}} \tag{29}$$

where T_{a} is the ambient temperature in °C.

The annual energy-saving ratio, R_{s}, is defined as the ratio of the annual energy saving by the proposed solar systems to the annual energy consumption by the conventional energy systems:

$$R_{\mathrm{s}} = \frac{E_{\mathrm{s}}}{E_{\mathrm{dem}} + \frac{Q_{\mathrm{hw,dem}}}{\eta_{\mathrm{eh}}} + \frac{Q_{\mathrm{sh,dem}}}{COP_{\mathrm{hp}}}} \tag{30}$$

2.2.2. Economic analysis

The annual operating cost savings, C_{s}, is defined as the difference between the current annual costs to cover all energy demand and the annual costs that the tourism sector would incur to cover all energy demand when the solar system was installed [15]:

$$C_{\mathrm{s}} = E_{\mathrm{cov}}c_{\mathrm{el}} + E_{\mathrm{exc}}s_{\mathrm{el}} + \frac{Q_{\mathrm{hw,cov}}}{\eta_{\mathrm{eh}}}c_{\mathrm{el}} + \frac{Q_{\mathrm{sh,cov}}}{COP_{\mathrm{hp}}}c_{\mathrm{el}} - C_{\mathrm{O\&M}} \tag{31}$$

where E_{exc} is the electricity excess exported to the grid and imported later via net metering, c_{el} is the electricity price (0.062 $/kWh in Fayoum), s_{el} is the electricity price for the net metering option (0.056 $/kWh in Fayoum), and $C_{\mathrm{O\&M}}$ are the operation and maintenance costs.

The payback time, *PBT*, defined as the period of time required to recover the investment costs of the proposed solar system, is calculated from Ref. [15]:

$$PBT = \frac{\ln\left[\frac{C_0(i_{\mathrm{F}}-d)}{C_{\mathrm{s}}} + 1\right]}{\ln\left(\frac{1+i_{\mathrm{F}}}{1+d}\right)} \tag{32}$$

where C_0 is the investment cost, i_{F} is the inflation rate (3 % in Africa [61]), d is the discount rate (5 % [62,63]).

The levelised cost of electricity, *LCOE*, is defined as [15]:

$$LCOE = \frac{C_0 + \sum_{i=1}^{n} C_{\mathrm{O\&M}}(1+i_{\mathrm{F}})^{i-1}(1+d)^{-i}}{\sum_{i=1}^{n} E(1+d)^{-i}} \tag{33}$$

where E is the net annual production of electricity or equivalent electricity converted from the thermal energy output: for a PV system, E is the actual electricity output since there is no thermal output; for a ST system, E is the equivalent electricity converted from the thermal energy output since there is no electricity output; for combined PV-ST and hybrid PVT systems, E is the sum of the actual electricity output and the equivalent electricity converted from the thermal energy output. A conversion factor of 0.98 is used from thermal energy of hot water to electricity, and Eq. (29) is used as a conversion factor from the thermal energy of space heating to electricity. Finally, n is the lifetime of the systems (25 years [64]).

The net present value, *NPV*, defined as the value of all the cash flows over the lifetime of an investment discounted to the present value, is used to estimate the profitability of the investment [25]:

$$NPV = \frac{C_{\mathrm{s}}}{d - i_{\mathrm{F}}}\left[1 - \left(\frac{1+i_{\mathrm{F}}}{1+d}\right)^{n}\right] - C_0 \tag{34}$$

The investment costs, C_0, are estimated from price lists available from solar retailers. The detailed costs for the main components in PVT-based systems, ST-based systems and PV systems are listed in Table 2. The investment costs for the combined PV-ST system are obtained by summing up the individual costs of the PV and ST sub-systems. The operation and maintenance costs ($C_{\mathrm{O\&M}}$) amount to 1 % of the total equipment costs for the PVT-based system, 0.6 % for the ST-based system, and 18 $/kW$_{\mathrm{p}}$ for the PV system [15]. The auxiliary heater costs are not considered as it is assumed that heat pumps and electrical heaters have already been installed as the backup systems.

2.2.3. Environmental potential

The annual CO_2 emission reduction of the proposed solar systems, *ER*, is assessed in the form of electricity due to the displaced electricity from the backup energy systems:

$$ER = \left(E_{\mathrm{cov}} + \frac{Q_{\mathrm{hw,cov}}}{\eta_{\mathrm{eh}}} + \frac{Q_{\mathrm{sh,cov}}}{COP_{\mathrm{hp}}}\right)f_{\mathrm{el}} \tag{35}$$

where f_{el} is the CO_2 emission factor of electricity (0.35 kgCO_2/kWh [15]).

The total environmental penalty cost-saving, *EPCS*, over the lifetime of the systems is [15]:

$$EPCS = \frac{ER \cdot c_{\mathrm{CO_2}}}{d - i_{\mathrm{F}}}\left[1 - \left(\frac{1+i_{\mathrm{F}}}{1+d}\right)^{n}\right] \tag{36}$$

Table 2
Cost breakdown of the solar heating and/or power systems.

System	Component	Value	Unit
PVT-based system	PVT collector	PVT-1: 451 [50] PVT-2: 358 [50] PVT-3: 588 [25] PVT-4: 440 [25]	$/collector
	Hydraulic components	446 [50]	$/set
	Expansion vessel	167 [50]	$/set
	Water storage tank	$1.04 \cdot V_t$ (l) + 908 [50]	$
	Piping	$(1.07 + 0.25 \cdot D_{pipe}) \cdot L_{pipe}$	$
	Heat transfer fluid	3.93 [50]	$/L
	Pump	$595 \cdot (P_{pump}/300)^{0.25}$	$
	Mounting	70	$/collector
	System installation	48	$/m^2
	$C_{O\&M}$	$0.01 \cdot C_0$ [15]	$
ST-based system[a]	ST collector	ST-1: 499 [51] ST-2: 1530 [52] ST-3: 518 [53] ST-4: 789 [54]	$/collector
	Mounting	56	$/collector
	System installation	29	$/m^2
	$C_{O\&M}$	$0.006 \cdot C_0$ [15]	$
PV system	PV module	PV-1: 186 [55] PV-2: 439 [56] PV-3: 164 [57] PV-4: 244 [58]	$/collector
	Inverter	240	$/kW$_p$
	System installation	$0.2 \cdot C_0$	$
	$C_{O\&M}$	18 [15]	$/kW$_p$

[a] All remaining components not listed here are the same as those in the PVT-based system.

where c_{co2} is the cost of unit CO_2 emission (0.01 $/kg$CO_2$ in Africa [65]).

2.3. Multi-objective optimisation algorithm

The optimisation of the solar systems aims to obtain optimal values for the decision variables (see below) under system constraints, using a solution algorithm to maximise or minimise objective functions. Energy systems should ideally have a good energetic performance and low costs. Therefore, a multi-objective optimisation is performed, maximising the annual energy-saving ratio (R_s) and minimising the payback time (*PBT*). The optimisations are performed using the stochastic NSGA-II solver [40], a widely used well-performing algorithm for multi-objective optimisation. By simultaneously optimising the R_s and *PBT*, a set of "non-dominated Pareto front" solutions can be obtained. For each of the solutions on the Pareto front, it is not possible to obtain a better value for one of the objectives without degrading the other. The algorithm regards the set of solutions within a Pareto front as equally optimal, or non-dominated. The important parameters of the genetic algorithm solver, such as the number of generations, the population size, the crossover fraction of variables, and mutation fraction of variables are 200, 50, 0.3 and 0.7, respectively.

Multi-objective optimisation simulations are performed for the PVT-based, the ST-based, and the PV-ST systems. For the PVT-based system and the ST-based system, the decision variables are the volume flow rate per collector ($\dot{V}_{f,u}$), the ratio of storage tank volume to total collector area (V_t/A_c), and the total collector area (A_c). For the PV-ST system, the decision variables further include the allocated area ratio between PV and ST in addition to the aforementioned variables. The constraints of the optimisation model are: (1) $0 < \dot{V}_{f,u} < 200$ L/h [14], (2) $0 < V_t/A_c < 200$ L/m^2 (typical value: 50 L/m^2 [15,50]), (3) $0 < A_c < 150$ m^2. Although no optimisation is performed for the PV system, investigations are conducted on the system performance by varying the total PV areas.

3. Description of the building selected for the case study

The evaluation of the different solar energy systems is performed for a hotel located in the city of Fayoum (Egypt) at a latitude and longitude of 29.3° N and 30.8° E. The site is characterised by a hot climate and an excellent solar resource, making it particularly suitable for the solar technologies considered in this study. The size of the solar system is limited by the maximum available roof area of 150 m^2. Fig. 2 shows the global horizontal solar irradiance and ambient temperature over a typical year at Fayoum. The data are obtained from the Photovoltaic Geographical Information System (PVGIS) database [66], using a typical meteorological year derived from the 10-year period between 2007 and 2016. As shown in Fig. 2, the solar irradiance on clear summer days can reach up to 1000 W/m^2. The annual average ambient temperature is 21 °C. With a total annual solar irradiance of up to 2300 kWh/m^2 and around 300 clear sunny days per year, Fayoum is particularly well suited for the deployment of solar energy technologies.

Fig. 3 shows the monthly electricity, space heating, and hot water demands of the considered hotel, obtained by aggregating half-hourly data. The annual electricity demand is 130 MWh/year and mainly consists of baseload consumption. Apart from the baseload electricity demands, the hotel has an annual space heating demand of 44 MWh/year and an annual hot water demand of 51 MWh/year. The space heating demand is currently covered by air-source heat pumps with an annual electricity consumption of 12 MWh/year. The hot water demand is satisfied by electrical heaters with an energy efficiency of 98 %, thus requiring 52 MWh of electricity annually. For all proposed solar systems, the required delivery temperatures are 55 °C for hot water and 60 °C for space heating.

The half-hourly meteorological data (solar irradiance, ambient temperature, and wind speed) and energy demand profiles (thermal demands for space heating and hot water heating, electricity demand) are inputs to the simulation over a year. To ensure a fair and consistent comparison, the techno-economic potentials of all proposed systems are assessed based on the same meteorological data, demand profiles, economic and environmental metrics.

4. Results and discussion

Multi-objective optimisations are performed to investigate the relationship between two competing techno-economic objectives: the payback time (*PBT*) and the annual energy-saving ratio (R_s). This section presents the resulting Pareto fronts for the solar systems introduced earlier. To further illustrate energetic performance, the aggregated annual energy demand coverage for different collector areas is also discussed.

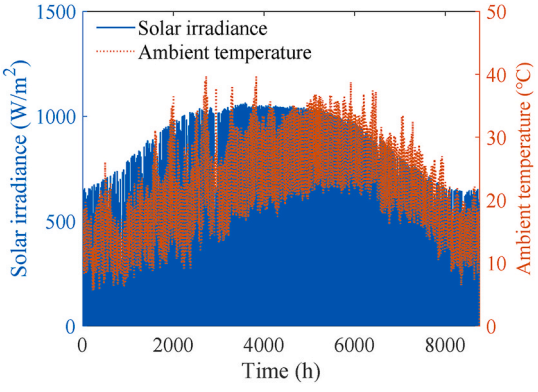


Fig. 2. Global horizontal solar irradiance and ambient temperature at the considered hotel at Fayoum, Egypt.

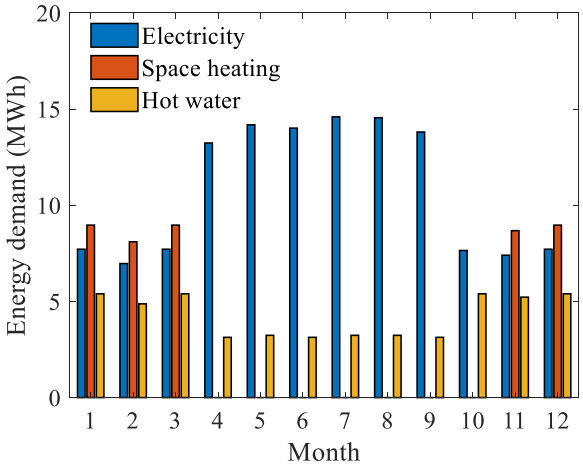


Fig. 3. Monthly electricity, space heating and hot water demands of the hotel in Fayoum, Egypt.

4.1. Hybrid photovoltaic-thermal systems

Fig. 4 shows the Pareto fronts from the techno-economic optimisation results for PVT-based solar systems for different PVT products. The decision variables are the volume flow rate per collector ($\dot{V}_{f,u}$), the ratio of storage tank volume to total collector area (V_t/A_c), and the total collector area (A_c). A clear trade-off between *PBT* and R_s is observed, as systems with lower R_s generally exhibit shorter payback times. The distribution of Pareto front solutions indicates that all the PVT candidates achieve similar maximum annual energy-saving ratios of 41–43 %. It is noted that the system with the lowest PVT collector price (PVT-2) is not able to achieve the lowest *PBT* at specific values of R_s, highlighting the importance of a comprehensive techno-economic assessment rather than selecting collectors based solely on upfront cost. In contrast, the solar system using the PVT-4 collector, which has an intermediate collector price (440 $/collector), outperforms the other candidates (highest price of 590 $/collector, lowest price of 360 $/collector) in terms of the *PBT* at equal values of R_s.

Fig. 5 shows the fractions of the building's annual energy demands covered by the PVT-based solar systems, including electricity demand coverage ($f_{el,cov}$), space heating demand coverage ($f_{sh,cov}$), and hot water demand coverage ($f_{hw,cov}$), for different areas. The annual energy demand covered by the PVT-based systems significantly increases as the area increases. For the example of the PVT-1 collector, when the system area increases from 20 m^2 to 150 m^2, $f_{el,cov}$ increases from 4.1 % to 21 %, $f_{sh,cov}$ from 2.6 % to 52 %, and $f_{hw,cov}$ from 40 % to 92 % due to the larger area available to collect solar energy. Across all PVT systems, the hot water demand can be covered to a greater extent than the space heating demand (max. 95 % *vs.* max. 60 %), while the electricity demand coverage ratio is the lowest (max. 31 %). The different PVT collectors have significantly different energy demand coverages due to their different electrical/thermal performance characteristics (listed in Table 1). For example, the PVT-4 collector has a higher electrical performance (η_{ref} = 18 %, β = -0.39 %) while displaying lower thermal efficiencies (η_0 = 47 %, a_1 = 9.5) due to the missing glass cover.

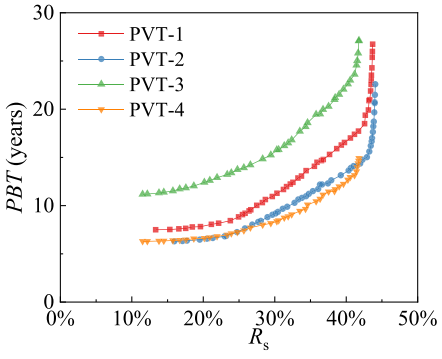


Fig. 4. Techno-economic multi-objective optimisation results for PVT-based solar systems with different PVT collectors. The different PVT collector products are marked by the corresponding case number as given in Table 1.

4.2. Solar-thermal systems

Fig. 6 compares the results of the multi-objective optimisation of the four ST systems, including low-cost evacuated-tube ST collector (ST-1), high-cost evacuated-tube ST collector (ST-2), low-cost flat-plate ST collector (ST-3), and high-cost flat-plate ST collector (ST-4). The decision variables are $\dot{V}_{f,u}$ V_t/A_c and A_c. The choice of the Pareto front should be based on a compromise between considerations of the *PBT* and R_s, i.e., the systems with the highest R_s also have the highest *PBT*. The flat-plate ST collectors (ST-3, ST-4) outperform the evacuated-tube ST collectors (ST-1, ST-2), reaching lower *PBTs* (min. 8.4 years *vs.* min. 13 years) and larger R_s (max. 29 % *vs.* max. 24 %). For the ST-based systems to remain profitable (*PBT* < 25 years), the annual energy-saving ratio must remain below approximately 22 %, 23 %, 27 % and 28 % of the total annual energy demand for the ST-1, ST-2, ST-3 and ST-4 systems, respectively. Among all ST collectors, ST-4 (790 $/collector), which has neither the lowest price (500 $/collector for ST-1) nor the highest price (1500 $/collector for ST-2), is the optimal option in terms of *PBT* and R_s. This result further demonstrates that detailed techno-economic optimisation across different product options is essential for identifying the optimal system configuration.

Fig. 7 shows annual space heating demand coverage ($f_{sh,cov}$) and hot water demand coverage ($f_{hw,cov}$) of the ST-based systems, for different collector areas and ST collectors. For all collectors, an increase in the total collector area from 20 m^2 to 150 m^2 results in a significantly higher coverage. For ST-4, for example, the space heating demand coverage increases from 3.9 % to 72 %, while the hot water demand coverage increases from 52 % to 98 %. For all the proposed ST systems, the higher fraction of thermal energy coverage is obtained with the hot water demand, as compared to that of the space heating demand at the same system area. Among the different ST collectors, it is noted that the high-cost flat-plate collector (ST-4) stands out from the other candidates in terms of energy coverage, while the low-cost evacuated-tube collector (ST-1) displays considerably lower thermal demand coverages for space heating (18 % *vs.* 72 % at 150 m^2) and hot water (82 % *vs.* 98 % at 150 m^2).

4.3. Photovoltaic systems

Fig. 8 illustrates the techno-economic performance of the different PV systems, showing the relationship between the annual energy-saving ratio (R_s) and the payback time (*PBT*) for varying collector areas (A_c). Four types of PV products are compared: a low-cost monocrystalline silicon (c-Si) module (PV-1), a high-cost c-Si module (PV-2), a low-cost polycrystalline silicon (p-Si) module (PV-3), and a high-cost p-Si module (PV-4). For all PV systems, R_s has only a minor influence on *PBT*, and the payback times of the PV-1, PV-2, PV-3, and PV-4 systems remain approximately constant: around 8.8 years, 13 years, 8.2 years, and 8.4 years, respectively. All the proposed PV systems are profitable, *i.e.*, *PBT* < 25 years. It should be noted that the *PBT* of the PV-2 system is considerably longer (around 63 % longer than other types of PV modules) due to the relatively higher collector price.

Fig. 9 shows the annual electricity demand coverage fractions of the proposed PV systems for different collector areas. Considering the maximum available roof area of 150 m^2, the maximum annual electrical power saved by the PV systems is limited to 32 % of the total annual

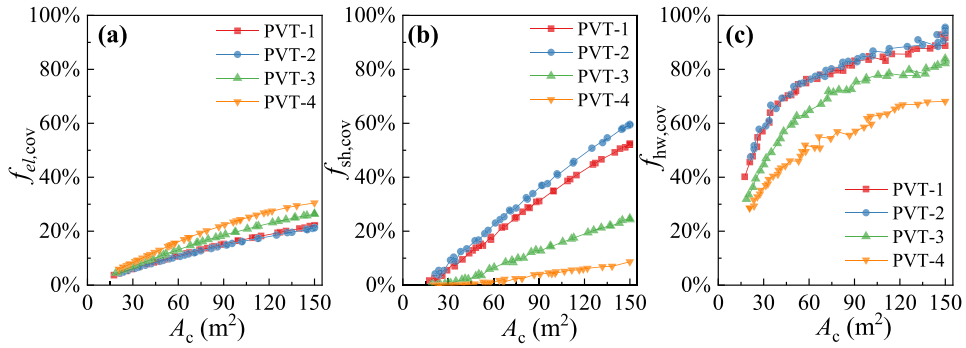


Fig. 5. Fraction of the annual energy demand covered by the PVT systems with different collector areas (A_c) and PVT collectors: (a) fraction of the electricity demand covered, $f_{el,cov}$, (b) fraction of the space heating demand covered, $f_{sh,cov}$, and (c) fraction of the hot water demand covered, $f_{hw,cov}$.

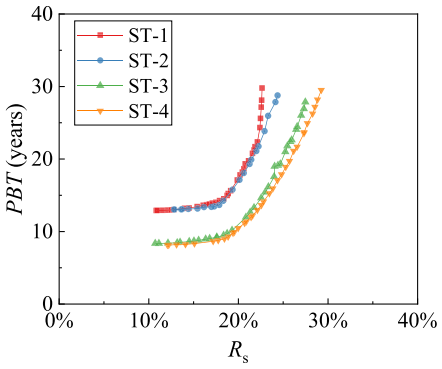


Fig. 6. Techno-economic multi-objective optimisation results for ST solar systems with different ST collectors, i.e., low-cost evacuated-tube ST collector (ST-1), high-cost evacuated-tube ST collector (ST-2), low-cost flat-plate ST collector (ST-3), and high-cost flat-plate ST collector (ST-4).

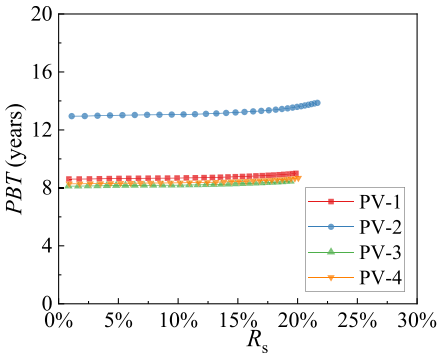


Fig. 8. Payback time (*PBT*) of PV systems for different annual energy-saving ratios (R_s): low-cost c-Si silicon PV module (PV-1), high-cost c-Si silicon PV module (PV-2), low-cost p-Si silicon PV module (PV-3), and high-cost polycrystalline silicon PV module (PV-4).

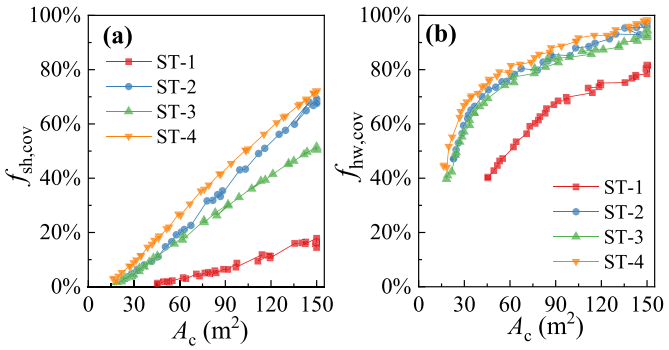


Fig. 7. Fraction of the annual energy demand covered by the proposed ST-based systems with different total collector areas (A_c) and ST collectors: (a) fraction of the space heating demand covered, $f_{sh,cov}$, and (b) fraction of the hot water demand covered, $f_{hw,cov}$.

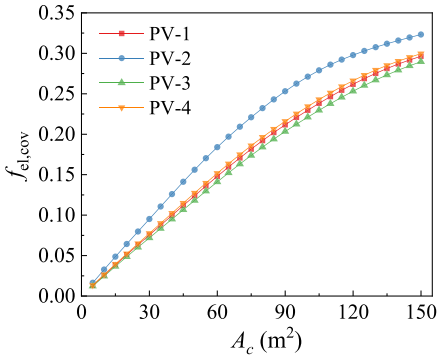


Fig. 9. Fraction of the annual electricity demand covered by the proposed PV systems for different total collector areas (A_c) and PV modules.

electricity demand. With the higher *PBT* of PV-2 as shown in Fig. 8, its annual electricity coverage ratio is also higher than that of other options due to the better electrical performance as shown in Table 1.

4.4. Combined photovoltaic and solar-thermal systems

Fig. 10 shows the multi-objective optimisation results for the PV-ST solar systems that combine the PV-1 module with different ST collectors, *i.e.*, PV-ST-1 (PV-1+ST-1), PV-ST-2 (PV-1+ST-2), PV-ST-3 (PV-1+ST-3), and PV-ST-4 (PV-1+ST-4). The decision variables are the $\dot{V}_{f,u}$, V_t/A_c, A_c, and the allocated area ratio between PV and ST. All PV–ST systems are found to be profitable, with payback times below 25 years. Among the PV-ST systems, PV-ST-4 appears as the best candidate due to its lower *PBT* as well as a higher limit of R_s. On the contrary, the PV-ST-1 system displays the worst techno-economic performance: R_s reaches a maximum of 29 % and the *PBT* is always longer than 10 years. Fig. 11 further demonstrates the optimal decision variables of A_c and allocated area ratio of PV to total area (A_{PV}/A_c) for the PV-ST-4 system. When increasing R_s, A_c is found to significantly increase first until it is limited by the available area (150 m^2), and A_{PV}/A_c increases first and then drops off. When $R_s < 16$ %, ST collectors should occupy a larger fraction of the total area ($A_{PV}/A_c < 50$ %), whereas for $R_s > 16$ %, a larger PV area becomes preferable ($A_{PV}/A_c > 50$ %).

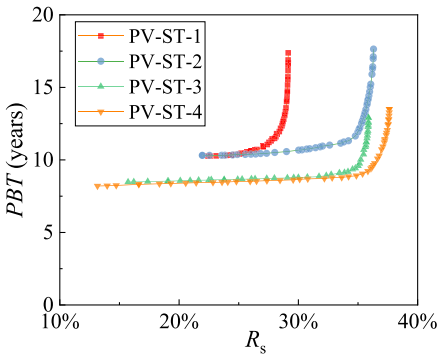


Fig. 10. Techno-economic multi-objective optimisation results for combined PV-ST solar systems: PV-1+ST-1 (PV-ST-1), PV-1+ST-2 (PV-ST-2), PV-1+ST-3 (PV-ST-3), and PV-1+ST-4 (PV-ST-4).

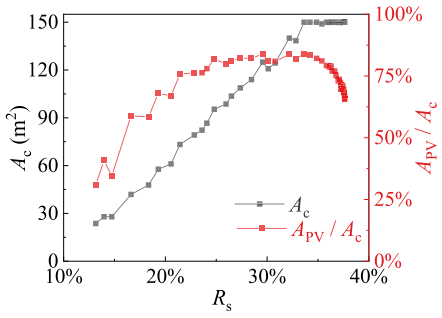


Fig. 11. Optimal decision variables of total collector area (A_c) and allocated area ratio of PV to total area (A_{pv}/A_c) for the PV-ST-4 system.

5. Further comparison between different systems

In this section, all proposed systems (PVT, ST, PV, and PV–ST heat and/or power systems) are compared in terms of energetic performance, economic potential, and environmental benefits. For this specific application, the techno-economic analyses are conducted under the current economic and environmental conditions relevant to the hotel in Fayoum, Egypt.

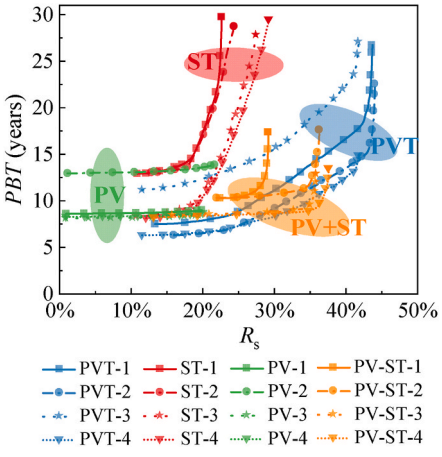


Fig. 12. Comparison of techno-economic multi-objective optimisation results for PVT-based, ST-based, PV, and PV-ST systems, with different solar collector products. The different solar collector products are marked by the corresponding case number as given in Table 1.

5.1. Trade-offs between energy savings and economic indicators

Fig. 12 shows the Pareto fronts of the techno-economic multi-objective optimisations of PVT, ST, PV, and PV-ST systems, with different solar collector products (marked by the corresponding case number as given in Table 1). When systems are compared at equal R_s, the PVT-4 system always has shorter PBT (down to 6.2 years) compared to the other solar systems considered in this work (except for PV-ST systems that stand out when the R_s is in the range from 32 % to 37 %). The shortest PBT of ST, PV, and PV-ST systems is between 8.1 and 8.6 years.

This finding contrasts with several published studies reporting longer payback times for PVT systems than for PV systems. To explain this, it is important to understand the different trade-offs: Although standalone PV and ST systems often exhibit higher electrical or thermal efficiencies than PVT systems, they must divide the available installation area between separate collectors. Therefore, if the total area is fixed, PVT systems often have a higher total energy generation (electrical + thermal) than standalone systems.

The referenced studies compare the *PBT*s of PV and PVT systems at equal collector areas. Therefore, the PVT systems have a higher *PBT* than the PV systems, while the R_s of the PVT systems are also higher than those of the PV systems. It is therefore more consistent to compare PV and PVT systems economically based on equal R_s (i.e., equal energy savings) as presented in this work. Besides, the results indicate that the PVT systems can achieve higher maximum energy savings. The maximum achievable energy-saving ratios are 43 % for PVT systems, followed by 34 % for PV–ST systems and 29 % for ST systems, while PV systems achieve the lowest maximum R_s of 22 %. It is noted that the combined PV-ST systems reach higher energy saving limits than standalone ST or PV systems.

Fig. 13 shows the relationship between the annual energy-saving ratio (R_s) and the *LCOE* of the proposed systems. The current electricity price (0.062 $/kWh) paid by the operator of the hotel is also given in the figure. The *LCOE*s of the proposed solar systems are below the current market electricity price over a wide range of R_s, implying they are profitable within their lifetimes. For equal R_s, the PVT system reaches the lowest *LCOE*. Taking R_s of 18 % as an example, the lowest *LCOE* of the PVT, ST, ST-PV, and PV systems are 0.029 $/kWh, 0.037 $/kWh, 0.038 $/kWh, and 0.040 $/kWh, respectively. These values correspond to a 35–53 % reduction relative to the current electricity price, though it is important to notice that the LCOE of all systems except the pure PV system is calculated based on both the electrical and the thermal energy output.

The results also indicate that the PV-ST systems and PVT systems are capable of reaching higher R_s (e.g., > 30 %) than the PV systems and ST systems. While the *LCOE* of the PV-ST-4 system is lower than those of the PVT systems over the range R_s = 32–37 %, the best PVT system still

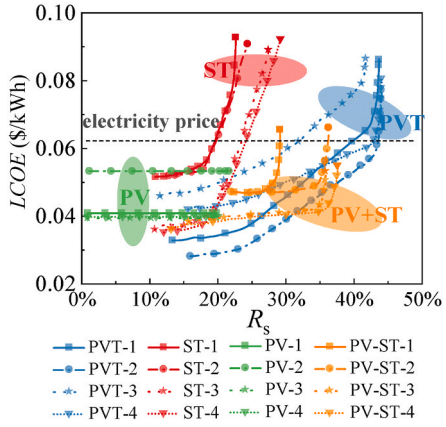


Fig. 13. *LCOE* of the proposed systems for different annual energy-saving ratio (R_s).

outperforms the PV-ST systems over a wide range of R_s. It can be concluded that for this particular case study, the PVT systems appear as more profitable alternatives compared to the other proposed systems. Incentives for renewable electricity and heating, which are expected to increase the profitability of the proposed solar systems, have not been considered in this work and are not necessary to make them economical.

Fig. 14 shows the investment costs of the proposed solar systems for different annual energy-saving ratios (R_s). As expected, increased investment costs are required for increasing R_s. For equal R_s, PVT systems have the lowest investment cost (except PV-ST systems that stand out when the R_s is in the range from 32 % to 37 %), followed by the PV-ST systems. The investment costs of the ST systems are the highest, but close to those of the PV systems.

Fig. 15 shows the net present value (*NPV*) of the proposed solar systems under different annual energy-saving ratios (R_s). The results show that each system exhibits a maximum *NPV* at a specific value of R_s: the best PV-ST system has the highest *NPV*, reaching about 42 k$ at R_s of 35 %; the maximum *NPV* of the best PVT system is higher than that of the best PV system (36 k$ *vs.* 23 k$), at R_s of 30 % and 22 % respectively; the lowest maximum *NPV* (22 k$) is achieved by the best ST system at R_s of 19 %. When comparing the *NPVs* of the solar systems at equal R_s, the best PVT system outperforms the other systems due to lower investment costs as shown in Fig. 14. It is also noted that the *NPVs* of the best ST system and best PVT system are negative when $R_s > 27$ % and $R_s > 43$ % respectively, implying that for these cases the proposed systems are not profitable within their lifetimes.

5.2. Evaluation of energy savings per collector area

To achieve cost-effective solar energy utilisation, it is necessary not only to reduce system costs but also to maximise the total energy savings per unit collector area. We therefore investigate the annual energy-saving ratio (R_s) of the proposed systems for different collector areas (A_c), as shown in Fig. 16. It should be stated that for the PV-ST systems, only the systems with better performance (PV-ST-3 and PV-ST-4) are considered here for a clearer comparison. It can be found that in this particular case, for equal system areas, the PVT systems have the potential to cover the largest amount of the energy demand, followed by the ST systems and the PV-ST systems, while the R_s of the PV systems are the lowest among all cases. Taking an area A_c of 150 m^2 as an example, the maximum R_s of the best PVT system is 43 %, which is larger than those of the best PV-ST system (34 %), ST system (31 %) and PV system (22 %). Previous comparative studies have often been conducted using equal collector areas, resulting in different R_s values and complicating economic comparisons. In contrast, the comparisons in this work are based on equal R_s for all the proposed systems, which provides a fairer economic comparison of the solar systems.

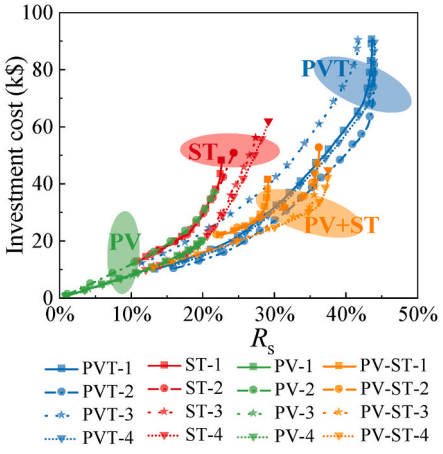


Fig. 14. Investment costs of the proposed systems for different annual energy-saving ratio (R_s).

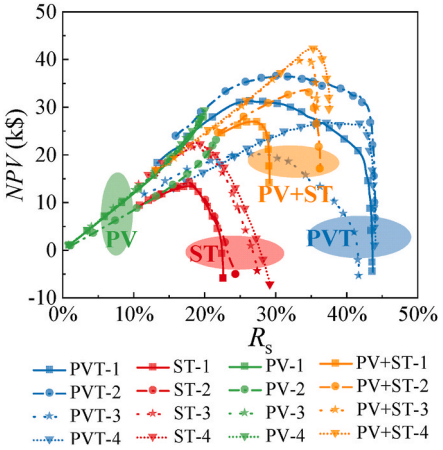


Fig. 15. Net present value (*NPV*) of the proposed systems for different annual energy-saving ratio (R_s).

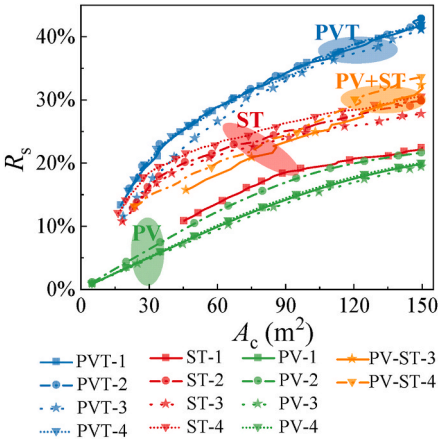


Fig. 16. Annual energy-saving ratio of the proposed systems for different collector areas (A_c).

5.3. Assessment of emission reduction potential

Fig. 17(a) shows the CO_2 emission reductions (*ER*) due to avoided consumption of electricity for different collector areas (A_c). For a given collector area, PVT systems achieve considerably higher emission reductions than the other technologies, reaching 31 tCO_2/year for the largest collector area of 150 m^2, due to the higher amount of saved energy per area as shown in Fig. 16. The *ER* of the best ST system is close to that of the best PV-ST system. PV systems have the lowest *ER* over a wide range of R_s due to the lower energy-saving per collector area, indicating the limited environmental benefits of the PV systems. Fig. 17 (b) shows the corresponding environmental penalty cost-saving (*EPCS*) due to reduced CO_2 emissions. The local carbon price in Egypt (0.01 $/kg$CO_2$) is used to assess the potential *EPCS* of the proposed solar systems. Similar to the trends of the *ER* in Fig. 17(a), the highest *EPCS* are achieved by the PVT systems over the whole range of collector areas. For example, at $A_c = 150$ m^2, the maximum *EPCS* reaches approximately 5900 $ for PVT systems, compared to less than 4800 $ for the other technologies. These findings suggest that PVT systems are very promising for the considered applications, and can help meet the targets set out in the national Sustainable Development Strategy: Egypt Vision 2030.

While the brief environmental analysis presented here is solely

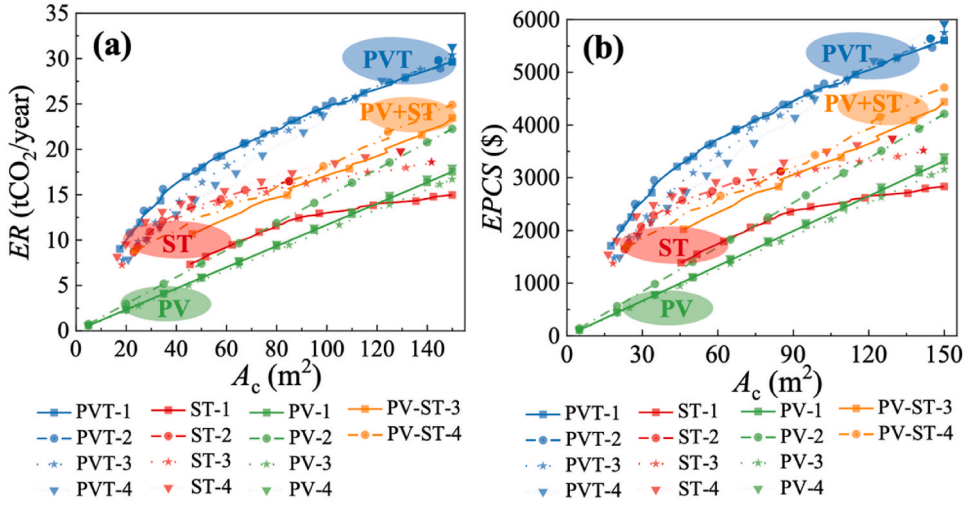


Fig. 17. (a) Annual CO_2 emission reduction (*ER*), and (b) total environmental penalty cost saving (*EPCS*) of the proposed systems for different collector areas (A_c).

focused on CO_2 emissions, it is important to acknowledge other environmental impacts such as energy use during construction, water consumption, and non-CO_2 emissions. A comprehensive life cycle assessment (LCA) to analyse these impacts would go beyond the scope of this paper. While the environmental impacts vary significantly depending on the system and location, it is noteworthy that several studies have demonstrated the benefits of solar energy systems, such as Liu et al. [67] for different regions in China and Carnevale et al. [68] for Italy. Parvez Mahmud et al. [69] found that solar PV systems generally perform better than solar thermal systems in terms of human health, ecosystem quality and climate change, but worse in terms of resource use, while Lamnatou et al. [70] review and compare the life cycle impacts of building-integrated solar energy systems.

5.4. Limitations and future work

While a comprehensive framework to compare different solar systems to provide electricity and heat has been developed, the analysis is subject to a number of limitations that should be addressed in future work. The solar energy systems are modelled using quasi-steady-state assumptions with half-hour time steps over the whole year. This modelling approach therefore prevents the capture of faster transient effects. Furthermore, the hot water storage tank is assumed to be fully mixed, while in reality ST systems are typically used with stratified storage tanks to increase their efficiency. Soriga and Badescu [71] showed that ST systems with stratified tanks are able to consistently deliver hot water at higher temperature compared to systems with mixed tanks. Wang et al. [72] found that the exergetic performance of a stratified tank is 10–15 % higher than that of a mixed tank. The assumption of a mixed tank in this study therefore represents a conservative approach that likely underestimates the potential of ST systems somewhat. This should be investigated in more detail in a future study.

Another limitation is that the study was only performed for one location and using a fixed electricity price. The sensitivity of the results towards these assumptions should be assessed to evaluate the applicability to other locations. In general, the energetic performance can be expected to be similar in other warm and solar-rich regions such as the Middle East, Southern Europe, Northern Africa, India, or Australia, as the demand profiles and availability of solar energy are similar. Cold and solar-rich regions will have a similar solar energy availability, but a higher thermal energy demand and a lower cooling demand, which will change the optimal system design. In regions with low solar availability, the potential of the systems evaluated in this study will be lower.

The economic model is based on fixed assumptions regarding electricity prices and collector costs. Both may change significantly in future, either due to technological improvements and/or larger and more efficient markets and streamlined supply chains leading to technology cost reductions, or due to policy changes affecting technology and energy costs. Higher electricity prices and lower technology costs will generally improve the economics of solar energy systems. The quantitative trade-off between the different technologies may change, for example, higher electricity prices will favour systems with PV while ST systems will not be affected. However, the general qualitative trends are expected to remain the same.

Finally, it would be desirable to validate the results presented here using data from real systems. The performance of the different solar collectors is modelled based on datasheets containing experimentally determined performance coefficients. However, evaluating the performance of the whole solar energy systems based on experimental data would be valuable, though it requires considerable effort and funding.

6. Conclusions

Four types of distributed solar energy systems, namely hybrid photovoltaic-thermal (PVT) systems, solar thermal (ST) systems, photovoltaic (PV) systems, and combined PV and ST systems (PV-ST), were assessed using a robust holistic comparison framework developed in this work. The focus was on the provision of heat and/or power to buildings in hot, solar-rich climatic regions. In this context, a hotel in Fayoum (Egypt) was selected as a representative case study to analyse the suitability of the proposed systems over an annual period of operation. Multi-objective optimisations were performed, maximising the annual energy-saving ratio and minimising the payback time of the systems. This approach enabled the identification of trade-offs between energetic performance and economic viability and allowed for a comprehensive comparison of the different solar technologies. Unlike many previous studies, which typically compare systems based on single designs and equal collector areas, the economic analysis in this work is conducted at equal annual energy-saving ratios, resulting in a more consistent and meaningful comparison.

The energetic assessment showed that electricity generation from all investigated solar systems covers less than one-third of the building's total electricity demand, however, the majority of the space heating and almost all of the hot water demands of the case study building can be covered by the systems. For the same installation area, the PVT systems were found to outperform the other proposed solar systems in terms of energy savings, while the PV systems had the lowest energy savings. Specifically, PVT systems achieve a maximum energy-saving ratio of 43 % when installed over the full available roof area of 150 m^2, followed by

the PV-ST systems (34 %) and the ST systems (29 %), while the lowest energy-saving ratio (22 %) is achieved by the PV systems.

In addition to having the highest energy savings, the PVT systems also have the best economic performance, reaching payback times as low as 6.2 years, which can be quite attractive for hotels and the buildings sector in general. PV-ST systems are the second best option, while pure ST or PV systems perform considerably worse both in terms of energy savings and economics. However, the economic assessments show that all proposed solar systems can be paid back within their lifetime (25 years), if they are properly sized and operated.

Overall, the proposed solar energy systems demonstrate strong decarbonisation potential and cost effectiveness, thus motivating further development for building applications in hot climate zones. In particular, as an emerging solar technology, PVT systems are found to be the superior solution among the alternatives in the present case study. Further efforts are required to boost their market penetration for promoting the global decarbonisation strategy.

CRediT authorship contribution statement

Jingyuan Xu: Writing – original draft, Software, Methodology, Investigation, Formal analysis, Data curation. **Jian Song:** Writing – review & editing, Resources. **Gan Huang:** Writing – review & editing, Investigation. **Matthias Mersch:** Writing – review & editing, Resources. **Kai Wang:** Writing – review & editing, Resources. **Christos N. Markides:** Writing – review & editing, Supervision, Project administration, Methodology, Funding acquisition, Conceptualization.

Declaration of competing interest

The authors declare that they have no known competing financial interests or personal relationships that could have appeared to influence the work reported in this paper.

Acknowledgements

This work was supported by an Institutional Links grant, ID 352350650, under the Newton-Mosharafa Fund partnership. The grant was funded by the UK Department for Business, Energy and Industrial Strategy and the Science and Technology Development Fund and delivered by the British Council. For further information, please visit www.newtonfund.ac.uk. This work was also supported by the UK Engineering and Physical Sciences Research Council (EPSRC) [grant number EP/R045518/1]. The authors would also like to acknowledge the helpful discussions with Dr. Andreas Olympios and Dr. Maria Herrando, and thank Suzan Abdelhady and Ahmed Shaban from Fayoum, Egypt, for their assistance in obtaining the energy demand data. The authors would like to thank the UK company Solar Flow Ltd. (www.solar-flow.co.uk). Data supporting this publication can be obtained on request from cep-lab@imperial.ac.uk. For the purpose of Open Access, the authors have applied a CC BY public copyright license to any Author Accepted Manuscript version arising from this submission.

Data availability

Data will be made available on request.

References

[1] https://www.iea.org/topics/buildings. [Accessed 19 April 2024].
[2] IRENAp. Global energy transformation: A roadmap to 2050. Abu Dhabi: International Renewable Energy Agency; 2018. p. 11. https://www.irena.org/-/media/Files/IRENA/Agency/Publication/2019/Apr/IRENA_Global_Energy_Transformation_2019.pdf.
[3] Polito F, Huang G, Markides CN. A building-integrated hybrid photovoltaic-thermal (PV-T) window for synergistic light management, electricity and heat generation. Adv Sci 2024:2408057.
[4] Hodes G. Perovskite-based solar cells. Science 2013;342(6156):317–8.
[5] Huang G, Wang K, Markides CN. Efficiency limits of concentrating spectral-splitting hybrid photovoltaic-thermal (PV-T) solar collectors and systems. Light Sci Appl 2021;10(1):1–14.
[6] REN21. Renewables 2024 global status report, renewables now. http://www.ren21.net; 2024.
[7] IRENA. Future of solar photovoltaic: deployment, investment, technology, grid integration and socio-economic aspects (A global energy transformation: paper). International Renewable Energy Agency, Abu Dhabi, 2019, p. 22. Available at: https://www.irena.org/-/media/Files/IRENA/Agency/Publication/2019/Nov/IRENA_Future_of_Solar_PV_2019.pdf.
[8] IRENA. Renewable power generation costs in 2019. International Renewable Energy Agency, Abu Dhabi, 2020, p. 70. Available at: https://www.irena.org/-/media/Files/IRENA/Agency/Publication/2020/Jun/IRENA_Power_Generation_Costs_2019.pdf.
[9] Bellos E, Tzivanidis C, Nikolaou N. Investigation and optimization of a solar assisted heat pump driven by nanofluid-based hybrid PV. Energy Convers Manag 2019;198:111831.
[10] Song Z, Ji J, Cai J, Li Z, Gao Y. Performance prediction on a novel solar assisted heat pump with hybrid Fresnel PV plus TEG evaporator. Energy Convers Manag 2020;210:112651.
[11] Olympios A, McTigue J, Antunez PF, Tafone A, Romagnoli A, Li Y, Markides CN. Progress and prospects of thermo-mechanical energy storage–A critical review. Progress in Energy 2021;3:022001.
[12] Mi Z, Chen J, Chen N, Bai Y, Fu R, Liu H. Open-loop solar tracking strategy for high concentrating photovoltaic systems using variable tracking frequency. Energy Convers Manag 2016;117:142–9.
[13] Ramos A, Guarracino I, Mellor A, Alonso-Álvarez D, Childs P, Ekins-Daukes NJ, Markides CN. Solar-thermal and hybrid photovoltaic-thermal systems for renewable heating. Imperial College London Grantham Institute, Briefing paper 2017;22.
[14] Herrando M, Markides CN, Hellgardt K. A UK-based assessment of hybrid PV and solar-thermal systems for domestic heating and power: system performance. Appl Energy 2014;122:288–309.
[15] Wang K, Herrando M, Pantaleo AM, Markides CN. Technoeconomic assessments of hybrid photovoltaic-thermal vs. conventional solar-energy systems: case studies in heat and power provision to sports centres. Appl Energy 2019;254:113657.
[16] Markides CN. Low-concentration solar-power systems based on organic Rankine cycles for distributed-scale applications: overview and further developments. Front Energy Res 2015;3:47.
[17] Li Z, Lu Y, Huang R, Chang J, Yu X, Jiang R, Roskilly AP. Applications and technological challenges for heat recovery, storage and utilisation with latent thermal energy storage. Appl Energy 2020:116277.
[18] Herrando M, Pantaleo AM, Wang K, Markides CN. Solar combined cooling, heating and power systems based on hybrid PVT, PV or solar-thermal collectors for building applications. Renew Energy 2019;143:637–47.
[19] Najjaran A, Freeman J, Ramos A, Markides CN. Experimental investigation of an ammonia-water-hydrogen diffusion absorption refrigerator. Appl Energy 2019;256:113899.
[20] Harraz AA, Haslam AJ, Mac Dowell N, Markides CN. Computer-aided molecular design of diffusion–absorption refrigeration modules for low-temperature solar collectors. Energy Convers. Manag. 2025;343:120067.
[21] Herrando M, Wang K, Huang G, Otanicar T, Mousa OB, Agathokleous RA, Markides CN. A review of solar hybrid photovoltaic-thermal (PV-T) collectors and systems. Prog Energy Combust Sci 2023;97:101072.
[22] Dupeyrat P, Ménézo C, Fortuin S. Study of the thermal and electrical performances of PVT solar hot water system. Energy Build 2014;68:751–5.
[23] Europe SP. EU market outlook for solar power 2019-2023. 2019.
[24] Wang K, Pantaleo AM, Herrando M, Faccia M, Pesmazoglou I, Franchetti BM, Markides CN. Spectral-splitting hybrid PV-thermal (PVT) systems for combined heat and power provision to dairy farms. Renew Energy 2020;159:1047–65.
[25] Herrando M, Simón R, Guedea I, Fueyo N. The challenges of solar hybrid PVT systems in the food processing industry. Appl Therm Eng 2021;184:116235.
[26] Winchester B, Huang G, Beath H, Sandwell P, Cen J, Nelson J, Markides CN. Lifetime optimisation of integrated thermally and electrically driven solar desalination plants. npj Clean Water 2024;7(1):65.
[27] Calise F, d'Accadia MD, Piacentino A. A novel solar trigeneration system integrating PVT (photovoltaic/thermal collectors) and SW (seawater) desalination: dynamic simulation and economic assessment. Energy 2014;67:129–48.
[28] Sakellariou EI, Axaopoulos PJ. Energy performance indexes for solar assisted ground source heat pump systems with photovoltaic-thermal collectors. Appl Energy 2020;272:115241.
[29] Xia L, Ma Z, Kokogiannakis G, Wang Z, Wang S. A model-based design optimization strategy for ground source heat pump systems with integrated photovoltaic thermal collectors. Appl Energy 2018;214:178–90.
[30] Wang K, Herrando M, Pantaleo AM, Markides CN. Thermodynamic and economic assessments of a hybrid PVT-ORC combined heating and power system for swimming pools. In: Heat powered cycles conference 2018; 2018. http://hdl.handle.net/10044/1/62245.
[31] Herrando M, Ramos A, Zabalza I, Markides CN. A comprehensive assessment of alternative absorber-exchanger designs for hybrid PVT-Water collectors. Appl Energy 2019;235:1583–602.
[32] Huang G, Curt SR, Wang K, Markides CN. Challenges and opportunities for nanomaterials in spectral splitting for high-performance hybrid solar photovoltaic-thermal applications: a review. Nano Mater Sci 2020;2(3):183–203.

[33] Huang G, Wang K, Curt SR, Franchetti B, Pesmazoglou I, Markides CN. On the performance of concentrating fluid-based spectral-splitting hybrid PV-thermal (PV-T) solar collectors. Renew Energy 2021;174:590–605.
[34] Eisapour M, Eisapour AH, Hosseini MJ, Talebizadehsardari P. Exergy and energy analysis of wavy tubes photovoltaic-thermal systems using microencapsulated PCM nano-slurry coolant fluid. Appl Energy 2020;266:114849.
[35] Mousa OB, Kara S, Taylor RA. Comparative energy and greenhouse gas assessment of industrial rooftop-integrated PV and solar thermal collectors. Appl Energy 2019; 241:113–23.
[36] Behar O, Sbarbaro D, Moran L. Which is the most competitive solar power technology for integration into the existing copper mining plants: photovoltaic (PV), concentrating solar power (CSP), or hybrid PV-CSP? J Clean Prod 2021;287: 125455.
[37] Thygesen R, Karlsson B. Simulation and analysis of a solar assisted heat pump system with two different storage types for high levels of PV electricity self-consumption. Sol Energy 2014;103:19–27.
[38] Mousa OB, Taylor RA, Shirazi A. Multi-objective optimization of solar photovoltaic and solar thermal collectors for industrial rooftop applications. Energy Convers Manag 2019;195:392–408.
[39] Good C, Andresen I, Hestnes AG. Solar energy for net zero energy buildings–A comparison between solar thermal, PV and photovoltaic–thermal (PV/T) systems. Sol Energy 2015;122:986–96.
[40] Song, L. (2025). NGPM – A NSGA-II program in MATLAB (Version 1.4). MATLAB Central File Exchange. Available at: https://www.mathworks.com/matlabcentral/fileexchange/31166-ngpm-a-nsga-ii-program-in-matlab-v1-4 (accessed 29 December 2025).
[41] European Standard EN 12975-2. Technical report, European Committee for standardisation (CEN). 2006.
[42] Freeman J, Hellgardt K, Markides CN. An assessment of solar-powered organic Rankine cycle systems for combined heating and power in UK domestic applications. Appl Energy 2015;138:605–20.
[43] Freeman J, Hellgardt K, Markides CN. Working fluid selection and electrical performance optimisation of a domestic solar-ORC combined heat and power system for year-round operation in the UK. Appl Energy 2017;186:291–303.
[44] Duffie JA, Beckman WA. Solar engineering of thermal processes. John Wiley & Sons; 2013.
[45] Schmidt EF. Wärmeübergang und druckverlust in rohrschlangen. Chem Ing Tech 1967;39(13):781–9.
[46] Rogers GFC, Mayhew YR. Heat transfer and pressure loss in helically coiled tubes with turbulent flow. Int J Heat Mass Tran 1964;7(11):1207–16.
[47] Fernández-Seara, J., Diz, R., Uhia, F. J., Sieres, J., and Dopazo, A. Thermal analysis of a helically coiled tube in a domestic hot water storage tank. Proceedings of HEFAT 2007 (5th International Conference on Heat Transfer, Fluid Mechanics and Thermodynamics), 2007, pp. 4–5.
[48] Bergman TL, Incropera FP, DeWitt DP, Lavine AS. Fundamentals of heat and mass transfer. John Wiley & Sons; 2011.
[49] Solartechnik Prüfung Forschung. Collector catalogue, CD, produced by Institut für Solartechnik SPF, Rapperswil, Berne. 2002.
[50] Herrando M, Ramos A, Freeman J, Zabalza I, Markides CN. Technoeconomic modelling and optimisation of solar combined heat and power systems based on flat-box PVT collectors for domestic applications. Energy Convers Manag 2018; 175:67–85.
[51] https://www.solardirekt24.de/vakuumroehrenkollektor-sonnenkollektor-euro therm-solar-20r-roehren-3-1-m2?c=2189 [accessed 19/April/2024].
[52] https://www.haustechnikonline.de/Solarbayer-Vakuum-Roehrenkollektor-CPC-18-Nero-Brutto-m2-326-400101801 [accessed 19/April/2024].
[53] https://www.wolf-online-shop.de/Junkers-Compact-Solarkollektor-FCC-2S-senkrecht::35326.html [accessed 19/April/2024].
[54] https://www.wolf-online-shop.de/Remeha-Flachkollektor-RemaSol-C-250-H-1000 16503::52371.html [accessed 19/April/2024].
[55] https://doi.org/10.5281/zenodo.4692648 [accessed 19/April/2025].
[56] https://www.buypvdirect.com/product-category/solar-pv-panles/perlight-mono-pv-panels [accessed 19/April/2024].
[57] http://www.windandsun.co.uk/products/Solar-PV-Panels/LG-Solar-PV-Panels#.YH81V-j0mix [accessed 19/April/2024].
[58] https://www.buypvdirect.com/product-category/solar-pv-panles/rec-solar-panels [accessed 19/April/2024].
[59] https://www.buypvdirect.com/product-category/solar-pv-panles/rec-solar-panels [accessed 19/April/2024].
[60] ASHRAE. HVAC systems and equipment handbook. Atlanta, GA, USA: American Society of Heating, Refrigerating and Air-Conditioning Engineers; 2020.
[61] http://www.inflation.eu/inflation-rates/historic-cpi-inflation.aspx. [Accessed 19 April 2024].
[62] Kim YD, Thu K, Bhatia HK, Bhatia CS, Ng KC. Thermal analysis and performance optimization of a solar hot water plant with economic evaluation. Sol Energy 2012; 86(5):1378–95.
[63] IEA. Projected costs of Generating Electricity 2015. Paris: IEA; 2015. https://www.iea.org/reports/projected-costs-of-generating-electricity-2015.
[64] Herrando M, Markides CN. Hybrid PV and solar-thermal systems for domestic heat and power provision in the UK: Techno-economic considerations. Appl Energy 2016;161:512–32.
[65] The World Bank. Carbon pricing dashboard. https://carbonpricingdashboard.worldbank.org. [Accessed 13 April 2025].
[66] https://ec.europa.eu/jrc/en/pvgis. [Accessed 19 April 2024].
[67] Liu C, Zhang Y, Zhao X. Comparative life cycle assessment of photovoltaic, solar-thermal, and hybrid PVT systems for building energy applications. Appl Therm Eng 2025;260:122331. https://doi.org/10.1016/j.applthermaleng.2025.122331.
[68] Carnevale E, Lombardi L, Zanchi L. Life cycle assessment of solar energy systems: comparison of photovoltaic and water thermal heater at domestic scale. Energy 2014;77:434–46. https://doi.org/10.1016/j.energy.2014.09.009.
[69] Mahmud MAP, Huda N, Farjana SH, Lang C. Environmental impacts of solar-photovoltaic and solar-thermal systems with life-cycle assessment. Energies 2018; 11(9):2346. https://doi.org/10.3390/en11092346.
[70] Lamnatou C, Chemisana D, Mateus R, Almeida MG, Silva SM. Review and perspectives on life cycle analysis of solar technologies with emphasis on building-integrated solar thermal systems. Renew Energy 2015;75:833–46. https://doi.org/10.1016/j.renene.2014.09.057.
[71] Soriga I, Badescu V. Performance of SDHW systems with fully mixed and stratified tank operation under radiative regimes with different degree of stability. Energy 2017;118:1018–34. https://doi.org/10.1016/j.energy.2016.10.137.
[72] Wang D, Liu H, Wang Y, Liu K, Liu Y, Gao M, Fan J. Thermal performance and evaluation of a novel stratified and mixed flexible transformation solar heat storage unit. Build Simulat 2023;16(10):1881–95. https://doi.org/10.1007/s12273-022-0930-z.